ELSEVIER

Journal of Chromatography B, 743 (2000) 31–40

JOURNAL OF CHROMATOGRAPHY B

www.elsevier.com/locate/chromb

Analysis of compression of polymer mushrooms using self-consistent field theory

B.M. Steels[a], F.A.M. Leermakers[b], C.A. Haynes[a,*]

[a]*Biotechnology Laboratory, Department of Chemical and Bioresource Engineering, 237 Wesbrook Building, The University of British Columbia, Vancouver, V6T 1Z3 Canada*

[b]*Department of Physical and Colloid Chemistry, Agricultural University Wageningen, Dreijenplein 6, 6703 HB Wageningen, The Netherlands*

Abstract

A number of new technologies, including new-generation biomaterials and chromatography resins, are based on passivation and modification of surfaces by terminally attaching polymer chains to the surface. However, little is known about these systems at the molecular level. In this work the compression of a single end-grafted polymer chain (or mushroom) by a disc of finite radius was investigated using a self-consistent field (SCF) lattice model. In accordance with results predicted using scaling theory [Subramanian et al., Europhys. Lett. 29 (1995) 285 and Macromolecules 29 (1996) 4045], the compressed chain undergoes a smooth escape transition. However, under the assumption of angular symmetry, a first-order escape transition of the end-grafted chain is not observed, suggesting that the formation of a tether is required for the predicted phase transition. Segment density distributions and compression energies are calculated in a cylindrical lattice. The energy required to compress a chain increases monotonically as the disc is moved closer to the surface and becomes independent of chain length at strong compressions where the work of compression involves only confinement of the tether joining the escaped chain fraction to the grafting point.

Keywords: Compression; Self-consistent field theory; Polymers

1. Introduction

Many important physical and chemical processes occur at the boundary between two phases. These processes can often be modified by attaching polymer chains to the interface. Such interfacial phenomena play an important role in, for example, chromatography, colloid or emulsion stabilization, and passivation of surfaces for biocompatibility. Hydrophobic interaction chromatography makes use of hydrophobic polymer chains grafted onto an inert support to enhance protein adsorption on column packing. Newer supports for size exclusion chromatography use colloidal particles with end-grafted polymer to separate proteins on the basis of size [3]. Flocculation of colloidal particles is often prevented by attachment of polymer chains on the particle surfaces to act as entropic bumpers [4]. Polymeric stabilization of liposomes for drug delivery is also under investigation. Polymer that is end-grafted to the surface of liposomes has been shown to reduce the rate at which they are cleared from circulation [5,6].

End grafting of polymer chains to a surface can

*Corresponding author.

0378-4347/00/$ – see front matter
PII: S0378-4347(00)00199-7

involve either covalent or ionic bonds. A block copolymer of structure A_nB_m, can also behave much like a grafted chain. For such systems, two regimes of surface coverage, leading to significantly different chain geometries have been proposed by de Gennes [7]: regime 1 corresponds to separate chain coils (mushrooms) and regime 2 to overlapping chains (brush). At low surface coverage, where the average separation between polymer chains is greater than the coil radius, R_g, no chain overlap will occur and a chain will form a 'mushroom'. At higher surface coverage, the chains will interact and, due to excluded volume effects, form a more extended layer, or 'brush'. This work specifically addresses the thermodynamic properties of regime 1, the polymer mushroom, by focusing on the compression of a single chain, grafted to a surface, by a disc of some finite radius, R_{disc}. Fig. 1 is a schematic of the grafted chain mushroom and associated dimensions in its (a) uncompressed (b) compressed, and (c) escaped states.

Because of the small size scale of an interfacial layer of polymer (10s to 100s of nanometers [8]), experimental measurement of polymer density distributions and repulsive forces is difficult. Density profiles of grafted layers have been successfully measured using small angle neutron scattering [9] (SANS), and force versus distance measurements have been made using the surface force apparatus [8] (SFA) and the atomic force microscope [10] (AFM). For the case of a single grafted polymer chain, however, it is unlikely that any experimental measurements are possible due to the prohibitively small length scales of polymer chains.

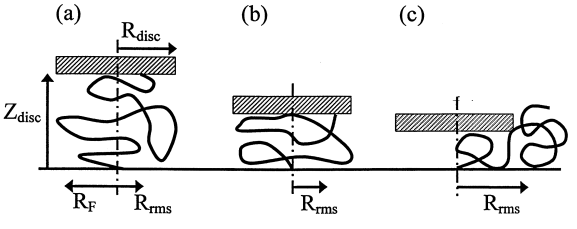

Fig. 1. Schematic diagram of a single end-grafted chain in (a) uncompressed (b) compressed, and (c) escaped states. The chain grafting point is at lattice position ($z = 0$, $r = 0$). Characteristic dimensions include: (i) disc position, Z_{disc}, (ii) disc radius, R_{disc} (iii) r.m.s. radius of segments from cylinder axis, R_{rms} and, (iv) Flory radius, R_F.

This difficulty in experimental characterization, combined with a desire to better understand polymer behavior at interfaces, has led to much work on modeling polymer at interfaces. Models for polymer have been derived from scaling theory [7], self-consistent field theory [11–13], and molecular dynamics simulations [14]. For the case of a single mushroom, scaling theory has recently been used to predict the behavior of a mushroom under compression. Subramanian [1,2] et al. predicted that a mushroom in a good solvent, compressed sufficiently by a disc of radius R_{disc}, which is greater than the coil radius R_g, undergoes a first-order escape transition upon compression, with hysteresis upon decompression. The authors suggest that a hysteretic first-order transition could be observed if a partly stretched chain has a lower free energy than one fully covered at equal compression. However, the scaling-theory model developed by Subramanian et al. is based on a number of simplifying assumptions, which in some instances are rather severe. For example, it is assumed that the Flory radius alone accurately describes the mushroom size. It is also assumed that as the chain is compressed it forms a string of blobs, and that the Flory radius accurately describes the blob size allowing calculation of the number of blobs. A further assumption is that the formation of each blob costs in energy about kT. Nevertheless, the blob model (and its more formal renormalisation extensions) remains the most accurate model for compressed mushroom conformations in good solvents.

In this work, a numerical self-consistent field model is used to study the compression of a single mushroom under a disc. The problem is cast in cylindrical coordinates to allow changes in chain segment densities to be determined in both the radial and surface-normal directions. Angular (θ) symmetry is assumed in the calculation. Relative to scaling thermodynamics, mean-field models based on the original work of Scheutjens and Fleer [11,12] provide a relatively detailed picture of the grafted-chain microenvironment. All thermodynamic quantities are calculated from equilibrium statistical thermody-

namics. The equilibrium segment density distribution is generated using a step-weighted walk, with the only restriction being the grafting point of the chain.

2. Self-consistent mean-field lattice theory

In the classical polymer solution theory by Flory [15] and Huggins [16] (FH theory), a chain is modeled as a random walk on a lattice. The solution volume is discretised into lattice sites of equal volume, and polymer chains and solvent molecules are modeled as connected and single segments, respectively. The occupancy of sites is determined by a mean-field approximation over the entire lattice where only the previous step of a chain is indexed when the next segment is added. In this way, FH theory gives an analytical expression for the combinational entropy change ΔS^c for mixing polymer chains with solvent. An enthalpy of mixing (ΔH) model based on regular solution theory [17] is often added to $-T\Delta S^c$ to allow estimation of the Gibbs' energy of mixing ΔG and the polymer and solvent chemical potentials. The ΔH model includes an interaction parameter, χ_{ij}, which gives half of the energy change associated with moving one segment of i from pure i into surroundings of pure j, while a segment of j travels from pure j to surroundings of pure i.

In order to model polymer adsorption at a surface, Scheutjens and Fleer (SF theory) developed a self-consistent-field lattice model based on FH theory, in which the mean field is allowed to vary in one dimension [11,12]. The model is able to account for the variation in polymer density in the direction normal to an interface. A statistical mechanical treatment of the lattice combined with step-weighted walk statistics gives the density distribution of polymer in each layer as well as thermodynamic information. An extension of their model gives the density distribution of end-grafted chains normal to a surface [18]. This model has been shown to give very good qualitative agreement with experimental measurements of polymer density distributions [19]. However, because of the increased complexity in the SF model, it requires a numerical solution.

A further extension of the SF model allows the mean field to vary in two dimensions. This is accomplished using a cylindrical geometry, in which density variations can be monitored in the normal direction (z) and the radial direction (r). This cylindrical mean field model has been used by Leermakers [20] to model lipid bilayer membranes containing other polymer molecules. Here, we apply the cylindrical mean-field type model to the description of the density distribution and thermodynamics of a single end-grafted chain under compression.

In the cylindrical lattice (Fig. 2), flat layers are numbered $z = 1, \ldots, Z_{max}$ in the normal direction and rings in the radial direction are numbered $r = 1, \ldots, R_{max}$. In each ring for a given layer z the lattice sites are considered to be indistinguishable and as a result of this mean field averaging is carried out. The end surface next to $z = 1$ is treated as an impenetrable surface at which the mushroom is grafted, and all other surfaces ($z = Z_{max}$, $r = R_{max}$) are treated as reflecting boundaries. The use of reflecting boundary conditions is appropriate, and simplifies the simulation, provided the boundary is set suffi-

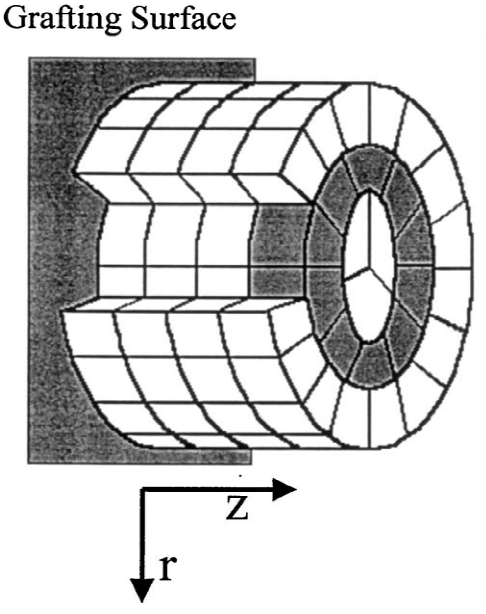

Fig. 2. Schematic diagram of the cylindrical lattice is shown with the coordinate directions, z and r. The mean field varies in each radial of the lattice as shown by the shaded radial.

ciently far from the grafting site to avoid the presence of chain or disc segments within the boundary region. The lattice was therefore of sufficient size to ensure that all lattice sites in contact with the radial boundary are occupied by solvent. In all calculations, the lattice is large enough that boundary effects on the chain are negligible. The number of sites per radial, r, in each layer is given by the area (in lattice units) of the radial:

$$L(r) = \pi\{r^2 - (r-1)^2\} \quad (1)$$

The outer surface area of a ring is then given by:

$$S(r) = 2\pi r \quad (2)$$

In order to evaluate the step-weighted random walk chain configurations, the step probability for a move from a given lattice site to any adjacent site needs to be known. We follow the same rules as Leermakers, and allow steps up (higher z), steps down or steps in the same layer. We also allow steps inward (lower r), steps outward or steps in the same radial shell and any combination of these two steps simultaneously (i.e. in and down).

Physically the lattice step probabilities are simply a consequence of the assumed geometry and are thus constants. In the normal direction, if a hexagonal lattice is assumed (12 nearest neighbors), the probability to step up or down a layer is simply $\lambda_1(z) = \lambda_{-1}(z) = 3/12$, corresponding to the number of nearest neighbors in the adjacent layers to layer z. The probability to stay in the same layer z is then $\lambda_0(z) = 6/12$. For steps inward and outward, the probabilities are made proportional to the lattice site surface area on the face that is crossed:

$$\begin{aligned} \lambda_{-1}(r) &= S(r-1)/L(r)*1/4 \\ \lambda_0(r) &= 1 - \lambda_{-1}(r) - \lambda_1(r) \\ \lambda_1(r) &= S(r)/L(r)*1/4 \end{aligned} \quad (3)$$

Thus, the probability to step down and outward simultaneously is given by:

$$\lambda_{-1,1}(z, r) = \lambda_{-1}(z)\ \lambda_1(r) \quad (4)$$

and likewise for all other step directions.

In order to generate the set of all chain conformations on the lattice, segments of type i are assigned a Boltzmann factor (free segment weighting factor):

$$G_i(z, r) = \exp(-u_i z, r)/kT) \quad (5)$$

The free segment-weighting factor is the preference a segment would feel to be in lattice position (z, r). It is based on the potential of mean force, $u_i(z, r)$, felt by the segment in that lattice position. The segment potential is composed of two contributions, a hard core potential, $u'(z, r)$, and an interaction potential, $u^{int}(z, r)$. The hard core potential is given by the Lagrange multipliers when the maximum term of the partition function is subject to the constraint that the lattice is filled. It therefore adjusts the segment potentials to ensure that the lattice space is completely filled without segment overlap.

The interaction potential, $u^{int}(z, r)$, is based on the local segment densities and χ_{ij} for unlike pair contacts:

$$\frac{u_i^{int}(z, r)}{kT} = \sum_j \chi_{ij}\{\langle\Phi_j(z, r)\rangle - \Phi_j^b\} \quad (6)$$

Here $\Phi_j(z, r)$ is the volume fraction of component j, in radial (z, r). The superscript b denotes the value in the bulk solution, which is zero for grafted components, and the angular brackets represent a step weighted average over all adjacent lattice sites. This is given in expanded notation by:

$$\langle\Phi_j(z, r)\rangle = \sum_{z'} \sum_{r'} \lambda_{z'-z,\, r'-r}(r\, z)\Phi_j(z', r') \quad (7)$$

In order to handle the connected nature of the chain segments, an end segment distribution function is generated using a recurrence formula. In this manner, the statistical weight of all conformations is systematically generated:

$$G_i(z, r, s+1|1) = G_i(z, r)\langle G_i(z, r, s|1)\rangle \quad (8)$$

The angular brackets again represent a step-weighted nearest neighbor average and $G_i(z, r)$ is the free-segment weighting factor for a segment of type i in radial (z, r). $G_i(z,r,s+1|1)$ gives the statistical weighting factor (chain end weighting factor) for a chain of $s+1$ segments to end in radial (z, r), after starting from an end segment with ranking 1. For the case of grafted chains, the chain end distribution function must be generated from each end of the chain (fixed and free) since inversion symmetry does not apply to end-grafted chains.

In order to graft a single chain to the center of the lattice at layer 1, the recurrence formula is started

from segment 1 with the restriction on that segment that:

$$G_i(z, r) = \exp(-u_i(z, r)/kT);\ z = 1, r = 1 \quad (9a)$$

$$G_i(z, r) = 0;\ \text{for all other } z, r \quad (9b)$$

This permanently grafts end-segment 1 of the chain to position (1,1) of the cylinder. The complementary chain-end distribution function is then generated (starting at the other end of the chain) with no restrictions on the remaining chain segments or the location of the free end. This is done using Eq. (8) from the starting point. The chain-end weighting factors for all chain conformations are computed and combined to give the segment density distributions, $\Phi_i(z, r)$:

$$\Phi_i(z, r) = C_i \sum_s \frac{G_i(z, r, s|1)G_i(z, r, s|N)}{G_i(z, r)} \quad (10)$$

Here, the summation is over all segment ranking numbers up to the full chain length, N. A normalization constant, C_i, is needed to transform the weighting factors to volume fraction. The normalization constant for chains fixed in the system (restricted equilibrium) is given by:

$$C_i = \frac{n_i}{\sum_z \sum_r L(r) g_i(z, r, N|1)} \quad (11)$$

In this way, coupling the end segment weighting factors for shorter chains generates the weighting factors for inner chain segments. The summation on s covers all possible segment positions in the chain and the normalization factor $G_i(z, r)$ eliminates double counting.

In this model three segment types have been used: polymer, solvent and disc segments. The polymer is considered a uniform homopolymer, and the disc is considered to have uniform properties, being composed of a fixed number of segments specified to fill the geometry chosen for it. The solvent is allowed to distribute freely in the system around both the grafted chain and the disc, which was fixed at a specified location for each calculation. The model also assumes that: (i) lattice sites are a constant volume and there is no volume change on mixing, and (ii) in applying mean field radials to the mushroom, the behavior of the polymer can be described without information about the radial chain trajectory (i.e. tether direction). This last assumption follows, in part, from the angular symmetry of the system.

The set of Eqs. (5), (6), (8) and (10) constitutes a large set of non-linear self-consistent equations, which can be solved numerically using the method of Leermakers [21]. The solution is based on the sum of volume fractions over segment type being unity and the hard core potential being independent of segment type once the correct solution is obtained. Because of the long computation time for large lattices, chain sizes were usually no more than several hundred segments.

3. Thermodynamics

Our procedure for calculating the energy required to compress an end-grafted chain with a disc follows the thermodynamic development in the original SF model [11,19]. Here, the result varies slightly to account for the radial non-uniformity in each lattice layer. The Helmholtz energy, A, can be calculated from the canonical partition function, Q, by:

$$A - A^* = -kT \ln (Q/Q^*) \quad (12)$$

The asterisk in Eq. (12) represents the reference state, which we specify as the pure, amorphous, unmixed components of the system. Because volume is constant in this lattice model, the Helmholtz energy is equal to the Gibbs energy.

The partition function can be written in terms of a combinational term and an energy U, term:

$$\ln (Q/Q^*) = \ln (\Omega/\Omega^*) - \left(\frac{U - U^*}{kT}\right) \quad (13)$$

In order to evaluate Q, both terms must be expressed as functions of the segment densities and segment potentials on the lattice. For first-order Markov-type chain statistics (random walk with backfolding allowed), Eq. (12) for the cylindrical geometry is similar to that for the original SF lattice with a one-dimensional variation in the mean field. We can therefore write the combinatorial term as:

$$\ln(\Omega/\Omega^*) = \sum_z \sum_r \sum_t L(r)\Phi_i(z,r) \times \left\{ \frac{\ln \Phi_i^b}{N_i} + \ln G_i(z,r) \right\} \quad (14)$$

Adding the energy term to Eq. (14) then gives us the complete Helmholtz energy:

$$\frac{(A-A^*)}{kT} = \sum_z \sum_r \sum_t L(r)\Phi_i(z,r) \left\{ \frac{\ln \Phi_i^b}{N_i} + \ln G_i(z,r) + \sum_{j>i} \chi_{ij} \langle \Phi_j(z,r) \rangle \right\} \quad (15)$$

In Eq. (15) the bulk volume fraction for solvent is unity, but for the grafted chain a substitution must be made since it is in restricted equilibrium [22]. It is possible to replace Φ_i^b for the grafted chain with an expression written in terms of the chain end weighting factors:

$$\Phi_i^b = \frac{n_i N_i}{\sum_z \sum_r L(r) G_i(z,r,N_i|1)} \quad (16)$$

where component i represents the grafted polymer.

For the energy calculation, the summation over all components, i, includes the polymer and solvent. The disc is considered completely uniform and its position unchanging. All unlike contacts are considered athermal so the last term of Eq. (15) is not required. It is possible however, to introduce interaction parameters simulating the case of poor solvent, or an attractive surface of the disc.

Finally, the energy change $A^{int}(z)$ due to compression of the mushroom is calculated by [23]:

$$A^{int}(z) = \{A - A^*\}(z) - \{A - A^*\}(\infty) \quad (17)$$

where the coordinate z represents the layer position of the leading edge of the disc. The disc is moved stepwise in the z-direction, toward the surface, and for each step the chain distribution is calculated in both dimensions.

4. Results and discussion

At low grafting density, the conformation of an end-grafted chain is based only on the impenetrable nature of the grafting surface and interactions of the chain with itself and solvent, assuming no other species are present. DeGennes [7] predicted that a single end-grafted chain in a good solvent will form a random coil, roughly in the form of a half sphere, with a radius of approximately the Flory radius, $R_F = aN^{3/5}$. In this equation, a represents the monomer length and N the number of monomers in the chain. In the lattice model, these parameters become the lattice dimension and the number of chain segments, respectively. Thus, a chain of 100 segments will have a Flory radius of about 16 lattice units. The root-mean-squared distance of segments from the cylinder axis:

$$R_{rms} = \left[\sum_r r^2 \frac{n(r)}{Nd} \right]^{1/2} \quad (18)$$

has also been calculated in this work in order to characterize the amount of spreading and escape a chain undergoes when compressed.

The fractional segment distribution in both the radial (r) and normal (z) directions is shown in Fig. 3 for an end-grafted chain of 100 segments in a good solvent ($\chi_{12} = 0$) under no compression. The Flory radius and R_{rms} of the coil as calculated in Eq. (18) are also shown in Fig. 3 for comparison. The number of segments in each radial $n(r)$ is calculated as:

$$n(r) = \sum_z L(r)\Phi(z,r) \quad (19)$$

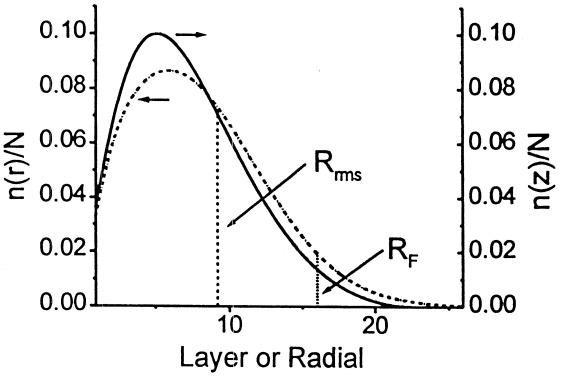

Fig. 3. Fractional segment distribution of a single end-grafted chain in the radial (r) (dash-dot line) and normal (z) (solid line) directions with $N = 100$ segments. Dashed line shows the root mean squared (rms) distance of segments from the center axis, R_{rms}, and dotted line shows the Flory radius, R_F.

which is simply the volume fraction $\Phi_i(z, r)$ multiplied by the number of lattice sites L in the radial r. The fractional distribution was then computed by normalizing Eq. (19) by the number of segments in the chain. In agreement with DeGennes' predictions [7], we find a maximum in the segment fraction a few layers from the surface in the normal direction. There is also a maximum in the segment fraction a few radials from the center. This is due to the fact that the inner radials have fewer lattice sites and can thus accommodate fewer segments despite having higher segment densities. The two curves approach zero at roughly the same distance, suggesting the chain forms roughly a half-sphere (or mushroom), spreading more in the radial than normal direction.

The segment density profile of a single end-grafted chain is shown in Fig. 4 (a). The density is highest at the point of grafting and drops off rapidly with distance from the surface. The graft density at (1,1) is about 0.4, which corresponds to slightly more than one segment in the π lattice sites of the first radial in layer 1. In Fig. 4 (b), a disc of radius 20 with a thickness of four layers has been placed in layer 2. The chain distribution around this disc is shown. It can be seen that the chain density becomes much higher in the outer radials ($r = 15–20$) of layer 1. A significant portion of the chain is escaped from under the disc and forms a smaller coil outside the edges of the disc.

The extent to which segments spread out in the radial direction under a compressing disc is proportional to R_{rms} (Eq. 18). The r.m.s. distance of segments from the center of the cylinder is shown in Fig. 5 for a chain of 100 segments compressed by two discs of different diameters. An important feature of Fig. 5 is that as the disc is made larger, more compression is required in order for chain escape. Consequently, the escape region is sharper (and therefore more similar to a first-order phase transition) due to the fact that more work is required to squeeze the chain to the edge of a larger disc. The escape of the chain under the disc of radius 20 is gradual, as seen by the solid line in Fig. 5.

Subramanian et al. [1,2] reported that for a disc larger than R_F a first-order escape transition is found. They argue that this transition is associated with an energy required to stretch the compressed polymer chain to the edge of the disc. For such a system (a disc of radius 30 compressing a polymer of Flory radius ca. 16), we observe a sharp, reversible transition, which is similar to (but does not completely conform to) a first-order escape transition. The

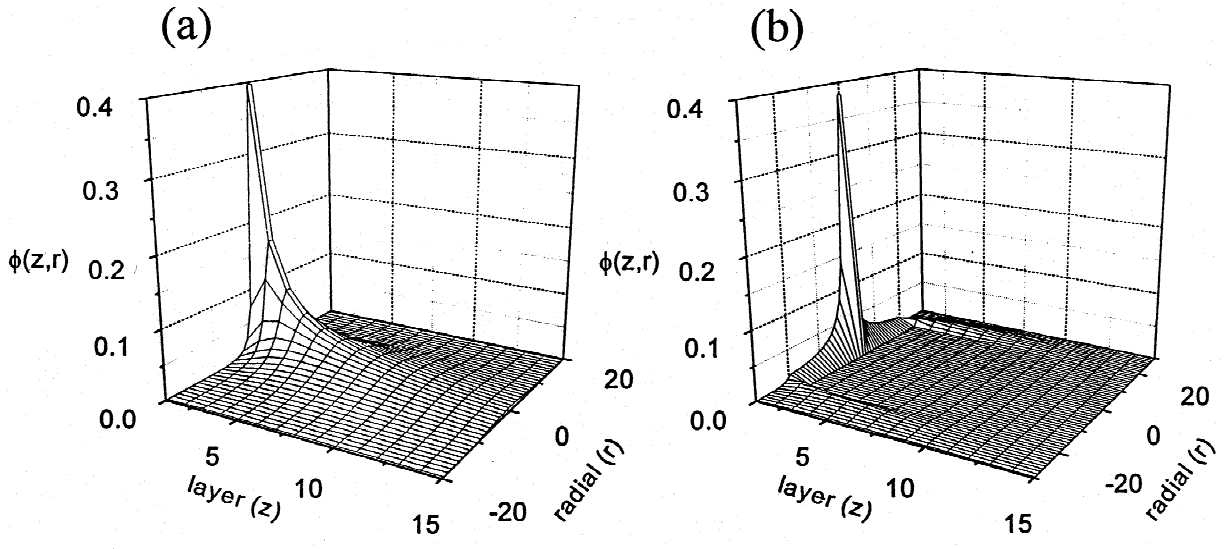

Fig. 4. Segment density distribution of a single end-grafted chain with $N = 100$. The chain is shown in (a) with no disc and in (b) with a disc of radius $R_{disc} = 20$ and thickness $Z_{disc} = 4$, sitting in layer 2 compressing the mushroom.

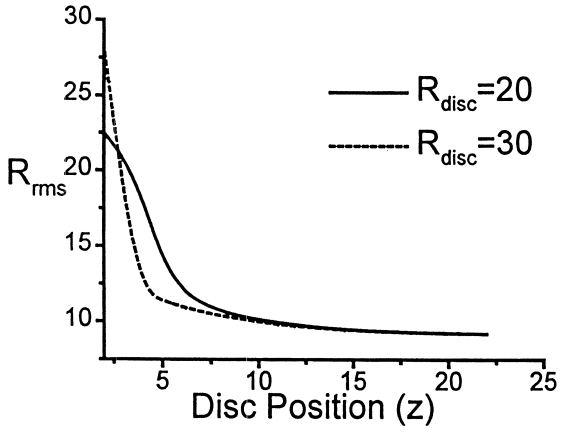

Fig. 5. Root mean squared distance of segments from the center of the cylinder, R_{rms}, is shown as the disc ($Z_{disc} = 4$) compresses a mushroom with $N = 100$. $R_{disc} = 20$ (solid), $R_{disc} = 30$ (dashed).

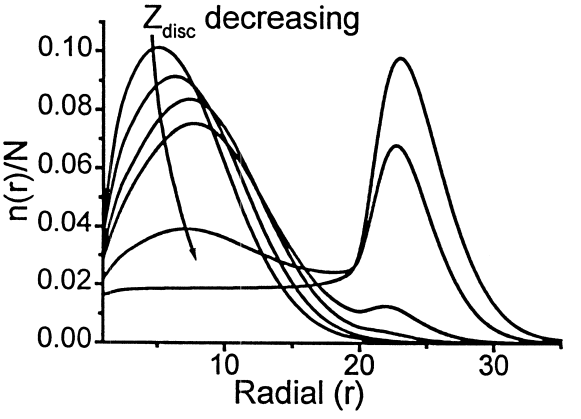

Fig. 6. Fractional segment distribution in the radial direction as a mushroom with $N = 75$ is compressed by a disc with $R_{disc} = 20$ and $Z_{disc} = 4$. The curves represent the disc in positions of $z = 16$, 8, 5, 4, 3, and 2.

scaling model of Subramanian et al. equates the calculated energy of two limiting cases in order to predict the compression at which a partially-escaped chain is in equilibrium with a compressed chain whose 2D Flory radius is close but not equal to the disc radius. The strongly compressed chain is modeled as a string of blobs, each with energy *kT*, and the escaped chain is modeled as a strongly stretched string of blobs (tether) with a fraction of the chain escaped. The fact that no such first-order transition is observed in our simulations suggests either that information about the transition between these two states is lost in the scaling model or, more likely, that the angular symmetry assumption in our model does not fully represent the highly compressed state. In particular, it suggests that the first-order phase transition requires that the compressed chain, upon escape, forms an angularly dependent tether (or string) and a mushroom at one side of the disc.

The segment fraction in each radial is shown in Fig. 6 for a chain of $N = 75$ segments compressed by a disc of radius $R_{disc} = 20$. This set of curves shows the results when the disc is placed in layer 16, 8, 5, 4, 3, and 2. Initial chain escape can be seen when the disc is placed in layer 5, and the fraction of segments escaped increases significantly as the disc is moved in further. The R_{rms} curve for compression (not shown) looks very similar to the dashed line in Fig. 5, but with a slightly less abrupt escape. It is interesting to note that with the disc in layer 2, the number of covered segments in each radial is about 1.5. Within the mean field approximation, we could interpret this result as formation of a strongly stretched tether under the disc with a large escaped portion, a picture consistent with the blob model and an escape transition. As the chain becomes longer, the tether becomes more strongly stretched and at infinite chain length, would become fully stretched to its limit of one segment per radial under a finite sized disc.

The energetic cost of compressing a mushroom has been calculated based on the loss of conformational entropy. Fig. 7 shows the compression energy for four different chain lengths. The curves represent compression under a disc of radius $R_{disc} = 20$, and the chain lengths are $N = 20$, 50, 100, and 200 segments. The curves are all monotonically increasing with compression. Comparing the calculated energy curves for long chains with that for the $N = 20$ chain, which cannot escape, shows that chain escape is not accompanied by changes in A^{int} characteristic of a first-order phase transition. Thus, although the model predicts a strong escape transition in terms of segment density profiles (see Fig. 4), it does not provide conclusive evidence of a first-order transition, suggesting that angular asymmetry (i.e. strong tethering) is an essential element of the

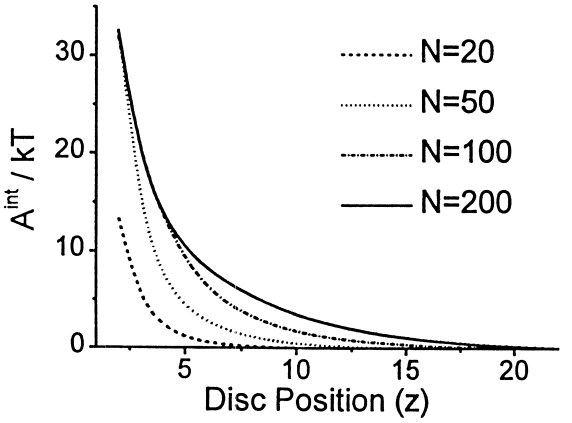

Fig. 7. Energy required to compress a mushroom with a disc of radius $R_{disc} = 20$ and thickness $Z_{disc} = 4$ for several chain lengths: $N = 20$ (dashed), $N = 50$ (dotted), $N = 100$ (dot-dash), $N = 200$ (solid).

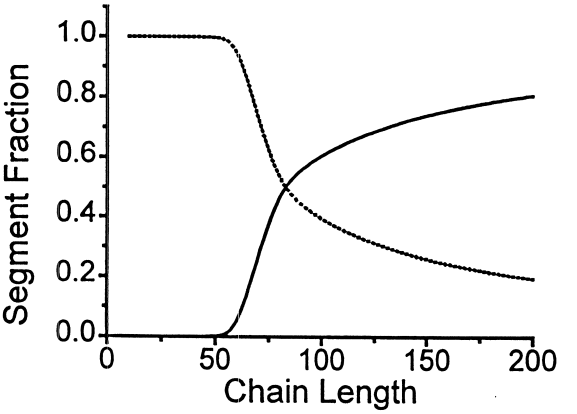

Fig. 8. Fraction of segments covered (dotted) and escaped (solid) from under a disc of radius 20, extending from $z = 3$ to the end of the cylinder (Z_{max}), as chain length is varied.

transition if it occurs. The only clear difference between the systems is a shift of the curve to the right (higher disc positions) with increasing chain length, due to the increased excluded volume repulsion of the compressed chain.

For the longer chains, $N = 50$, $N = 100$ and $N = 200$, it can be seen that portions of the energy curves coincide at high compression. The energy curves for $N = 50$ and $N = 100$ overlap on the $N = 200$ curve at a point where the shorter chains have just started to escape. Further compression therefore involves only the work of compressing the polymer tether, which is independent of chain length.

In order to investigate the chain escape further, chain length was varied under a fixed disc of radius $R_{disc} = 20$. For simplicity, the disc extended from layer 3 to $z = Z_{max}$, since for discs where $R_{disc} > R_F$ the thickness of the disc has no influence on chain escape energetics or segment density profiles. Fig. 8 shows the fraction of segments covered by the disc (dotted) and the fraction of segments escaped (solid) from under it. The onset of escape occurs at just over 50 segments, indicating that the critical length for escape is significantly larger than the minimal length for escape. This is not surprising since the escape is primarily driven by the increase in conformational entropy of those segments within the escaped mushroom.

5. Conclusions

The compression of a single end-grafted chain by a disc of finite radius was investigated using a self-consistent mean-field model. Chain segment distributions for uncompressed chains (mushrooms) and compressed chains are quantitatively and qualitatively consistent, respectively, with results predicted by de Gennes [7]. However, in contrast to more recent work using a model based on scaling theory [1,2] we find no first-order escape transition when a chain is compressed. This disparity may be due to the assumption of angular symmetry used in this work, indicating that stretching of the chain in a random direction is an essential element of the transition. Based on this model, the chain appears to be squeezed out from under the disc, often abruptly, as the disc approaches the surface. The energy required to compress the mushroom increases with compression and becomes independent of chain length following chain escape.

References

[1] G. Subramanian, D.R.M. Williams, P.A. Pincus, Europhys. Lett. 29 (1995) 285–290.
[2] G. Subramanian, D.R.M. Williams, P.A. Pincus, Macromolecules 29 (1996) 4045–4050.

[3] D. Brooks, V.J. Muller, Molec. Recog. 9 (1996) 697–700.
[4] D.H. Napper, Polymeric Stabilization of Colloidal Dispersions, Academic Press, New York, 1983.
[5] M.C. Woodle, D.D. Lasic, Biochim. Biophys. Acta 1113 (1992) 171–199.
[6] P.G. de Gennes, Macromolecules 13 (1980) 1069–1075.
[7] P.G. de Gennes, Macromolecules 13 (1980) 1069–1075.
[8] H.J. Taunton, C. Toprakcioglu, L.J. Fetters, J. Klein, Macromolecules 23 (1990) 571–580.
[9] T. Cosgrove, K. Ryan, Langmuir 6 (1990) 136–142.
[10] G.J.C. Brathwaite, A. Howe, P.F. Luckham, Langmuir 12 (1996) 4224–4237.
[11] J.M.H.M. Scheutjens, G.J. Fleer, J. Phys. Chem. 83 (12) (1979) 1619–1635.
[12] J.M.H.M. Scheutjens, G.J. Fleer, J. Phys. Chem. 84 (1980) 178–190.
[13] S.T. Milner, Science 251 (1991) 905–914.
[14] M. Murat, G.S. Grest, Macromolecules 29 (1996) 8282–8284.
[15] P. Flory, Principles of Polymer Chemistry, Cornell University Press, Ithaca, NY, 1953.
[16] M.L. Huggins, J. Phys. Chem. 46 (1942) 151.
[17] J.M. Prausnitz, R.N. Lichtenthaler, E.G. de Azevedo, Molecular Thermodynamics of Fluid-phase Equilibria, 2nd ed., Prentice-Hall, Englewood Cliffs, NJ, 1986.
[18] T. Cosgrove, T. Heath, Macromolecules 20 (1987) 1692–1696.
[19] G.J. Fleer, M.A. Cohen Stuart, J.M.H.M. Scheutjens, T. Cosgrove, B. Vincent, Polymers at Interfaces, Chapman and Hall, London, 1993.
[20] F.A.M. Leermakers, J.M.H.M. Scheutjens, Lyklema, J. Biochim. Biophys. Acta, 1024 (1990) 139–151.
[21] F.A.M. Leermakers, J.M.H.M.J. Scheutjens, Chem. Phys. 89 (1988) 3264–3274.
[22] J.M.H.M. Scheutjens, G.J. Fleer, Macromolecules 18 (1985) 1882–1900.
[23] B. Van Lent, R. Israels, J.M.H.M. Scheutjens, G.J. Fleer, J. Colloid Interface Sci. 137 (1990) 380–394.